

A STUDY ON THE PERFORMANCE OF LINEAR ACTUATORS WITH SHAPE MEMORY ALLOY HELICAL SPRINGS

Juliana Hoyer Insaurrauld Pereira, julihoyer@yahoo.com.br

Cristina Gomes de Souza, cgsouza@cefet-rj.br

Pedro Manuel Calas Lopes Pacheco, calas@cefet-rj.br

CEFET/RJ – PPTEC – Av. Maracanã, 229 – Bloco E – 5º andar - 20271-110 - Rio de Janeiro - RJ - Brazil

Abstract. *Technologic evolution in the last years permitted the development of new actuation and control systems using intelligent materials as shape memory alloys (SMAs). SMAs are metallic materials that have the capability to generate large strains and loads associated to phase transformation induced by stress or temperature. Because of such properties, SMAs have found a number of applications in different areas as actuation systems. The increasing number of scientific publications and patents associated to actuators technology registered in ISI/Web of Science and Derwent Innovations Index databases show that this subject is attracting much technological interest. Among these devices SMA actuators have received large attention. To evaluate the performance of linear actuators with shape memory alloy helical springs, a simplified model for shape memory alloy helical springs is presented, in which the shear behavior is based on a constitutive model with assumed transformation kinetics. The proposed model considers that the shear stress and volumetric fraction phase present a homogeneous distribution along the wire cross section. The resulting coupled problem is solved using a split operator scheme that leads to three uncoupled problems: Thermal Problem, Phase Transformation Problem and Mechanical Problem. Thermomechanical characterization of the SMA helical springs is obtained through load-displacement tests performed using a tensile test device. Numerical results show that the model is in close agreement with those obtained by experimental tests, indicating that the model can be used to represent the behavior of SMA helical springs actuators. Finally several conditions are analyzed with the proposed model to assess the main characteristics of SMA helical springs actuators performance.*

Keywords: *shape memory alloys, actuators, helical springs, modeling*

1. INTRODUCTION

Shape memory alloys (SMAs) have the capability to generate large strains associated to phase transformation induced by stress and/or temperature variations (Hodgson *et al.*, 1992; Rogers, 1995). During the phase transformation process of a SMA component large loads and/or displacements can be generated in a relatively short period of time making this component an interesting mechanical actuator. Two phases are present: martensite and austenite (Zhang *et al.*, 1991). For lower temperatures, below a critical temperature, twinned martensite phase is the only stable phase in a stress-free state, whereas detwinned martensite is associated to the presence of a stress field above a critical stress. Several alloys can develop strains associated to phase transformation but only those that can develop large strains are of commercial interest, as nickel-titanium (NiTi) and copper base alloys (CuZnAl and CuAlNi).

These remarkable characteristics have been responsible for the increasing interest in different applications varying from biomedical to aerospace industry. Machado and Savi (2003) make a review on the most relevant SMA applications within orthodontics and biomedical areas. SMAs are ideally suited to be used in engineering applications as self-actuating fasteners, thermally actuator switches, seals, connectors and clamps (van Humbeeck, 1999; La Cava *et al.*, 2000). Moreover, aerospace technology is also exploiting SMA properties in order to build self-erectable structures, stabilizing mechanisms, solar batteries, non-explosive release devices and other possibilities (Denoyer *et al.*, 2000; Pacheco and Savi, 1997). Micromanipulators and robotics actuators have been conceived employing SMAs properties to mimic the smooth motions of human muscles (Webb *et al.*, 2000; Rogers, 1995; Kibirkstis *et al.*, 1997; Chang-jun *et al.*, 2004). Furthermore, SMAs are being used as actuators and absorbers for vibration and buckling control of flexible structures (Rogers, 1995; Williams *et al.*, 2002; Elzey *et al.*, 2005; Shi *et al.*, 2005).

Figure 1a presents a stress-strain curve for the shape memory effect at a constant temperature. The nonlinear behavior in the loading process ($A \rightarrow B$) is associated to phase transformation related to the conversion from twinned to detwinned martensite. After the unloading process (C), some amount of residual strain remains (ϵ_R), meaning that the reverse transformation, from detwinned to twinned martensite, is not completed. The shape memory effect takes place by heating the alloy, which controls the transformation from detwinned martensite to austenite and promotes the residual strain recovery. Figure 1b presents a diagram that illustrates the shape memory effect. A_S and A_F are the temperatures at which the formation of austenite starts and ends, respectively. M_S and M_F are the temperatures at which the formation of martensite starts and ends, respectively.

The complex thermomechanical behavior of SMAs makes their modeling a difficult task. This may introduce difficulties in the evaluation of SMA applications. SMA springs are an important actuating device that can be used in different applications. There are some efforts to model the SMA helical springs thermomechanical behavior (Toi *et al.*, 2004, Savi and Braga, 1993; Tobushi and Tanaka, 1991). In the present contribution, it is proposed a model that may be

useful for engineering purposes. Basically, a constitutive model originally proposed for one-dimensional tensile-compressive behavior (Brinson, 1993) is employed to describe the shear behavior. Afterwards, it is developed a SMA helical spring model by assuming that the shear stress and volumetric fraction phase present a homogeneous distribution along the wire cross section. An experimental apparatus is developed in order to characterize the thermomechanical behavior of SMA helical springs through load-displacement tests and numerical simulations are carried out showing that the proposed model is in close agreement with experimental tests. Finally several conditions are analyzed with the proposed model to assess the main characteristics of SMA helical springs actuators performance.

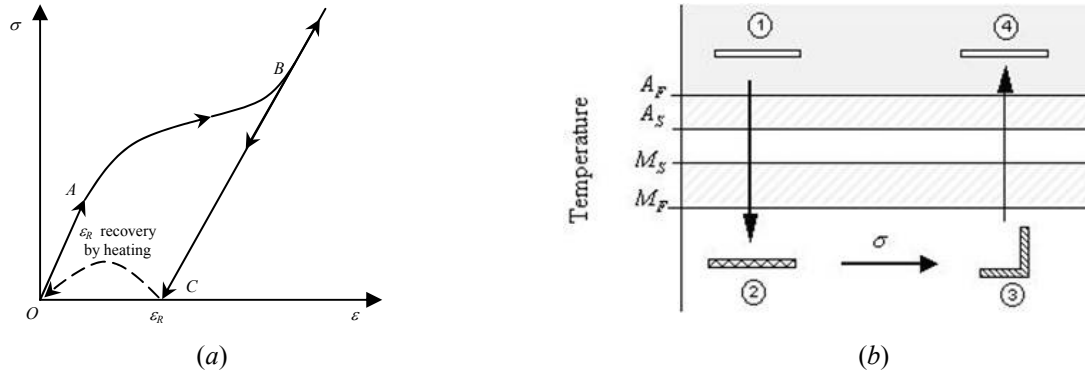


Figure 1. Shape memory effect. Stress-strain curve (a) and a diagram to illustrate the shape memory effect (b).

2. CONSTITUTIVE MODEL

SMA's thermomechanical behavior can be described by different constitutive models. Paiva e Savi (2006) present an overview of some constitutive models for SMA's. In this work, the model with assumed transformation kinetics proposed by Brinson (Brinson, 1993) is considered. It is an one-dimensional model which assumes the kinetics of the phase transformation establishing a relationship between the martensitic fraction, β , with temperature and one-dimensional strain, ε . Brinson's model considers that martensitic fraction is composed by two distinct parts: temperature induced martensitic fraction, β_T , and stress induced martensitic fraction, β_S . Therefore $\beta = \beta_T + \beta_S$.

Although this one-dimensional constitutive model is originally proposed to describe tension-compression behavior, it has been noted that experimental torsion test curves presented in different references (Jackson *et al.*, 1972; Manach and Favier, 1997) indicate that these curves are qualitatively similar to those obtained in tension tests performed in Ni-Ti and other SMA's. Based on this observation, this constitutive model is employed to describe the pure shear stress states, replacing the stress, strain, and elastic modulus, respectively, by the shear stress, τ , shear strain, γ , and shear modulus, G . With this assumption, it is possible to obtain a complete set of constitutive equations that describes the thermomechanical behavior of SMA's. The shear stress evolution is represented by the following equation:

$$\dot{\tau} = G\dot{\gamma} + \alpha\dot{\beta}_S \quad (1)$$

where $G = G_M + \beta(G_A - G_M)$ is the shear modulus and α is a coefficient associated with phase transformation. G_A is the austenite shear modulus and G_M is the martensite shear modulus.

The phase transformation are assumed to be determined by the current values of stress and temperature, $\beta = \beta(\tau, T)$. For $T > M_S$ the transformation from austenite to detwined martensite may be described by:

$$\beta_S = \frac{1 - \beta_{S0}}{2} \cos \left\{ \left(\frac{\pi}{\tau_S^{CRIT} - \tau_f^{CRIT}} \right) \left[\tau - \tau_f^{CRIT} - C_M(T - M_S) \right] \right\} + \frac{1 + \beta_{S0}}{2} ; \quad \beta_T = \beta_{T0} - \frac{\beta_{T0}}{1 - \beta_{S0}} (\beta_S - \beta_{S0}) \quad (2)$$

where τ_S^{CRIT} and τ_f^{CRIT} are critical stress for martensitic transformation start and finish, C_M is a positive constant and β_{T0} and β_{S0} represents the volumetric fractions of martensite before transformation begins to take place. This equation holds for $\tau_S^{CRIT} + C_M(T - M_S) < \tau < \tau_f^{CRIT} + C_M(T - M_S)$. For $T < M_S$ and $\tau_S^{CRIT} < \tau < \tau_f^{CRIT}$:

$$\beta_S = \frac{1 - \beta_{S0}}{2} \cos \left[\frac{\pi}{\tau_S^{CRIT} - \tau_f^{CRIT}} (\tau - \tau_f^{CRIT}) \right] + \frac{1 + \beta_{S0}}{2} ; \quad \beta_T = \beta_{T0} - \frac{\beta_{T0}}{1 - \beta_{S0}} (\beta_S - \beta_{S0}) + \Delta T \quad (3)$$

$$\text{where } \Delta T = \begin{cases} \left\{ \frac{1-\beta_T}{2} \left[\cos \left[\frac{\pi}{M_S - M_F} (T - M_f) \right] + 1 \right] \right\} & \text{for } M_F < T < M_S, T < T_0 \\ 0 & \text{otherwise} \end{cases}$$

The reverse transformation occurs for $T > A_S$ and $C_A(T - A_F) < \tau < C_A(T - A_S)$, where C_A is a positive constant, and is described by:

$$\beta_S = \frac{\beta_S}{2} \left\{ \cos \left[\frac{\pi}{A_f - A_S} \left(T - A_S - \frac{\tau}{C_A} \right) + 1 \right] \right\} ; \quad \beta_T = \frac{\beta_{T0}}{2} \left\{ \cos \left[\frac{\pi}{A_f - A_S} \left(T - A_S - \frac{\tau}{C_A} \right) + 1 \right] \right\} \quad (4)$$

3. SHAPE MEMORY ALLOY HELICAL SPRING

Modeling of the restoring force produced by a SMA spring is done considering a helical spring with diameter D , built with N coils with a wire diameter d (Fig. 2).



Figure 2. Helical spring.

It is assumed that the longitudinal force, F , is resisted by the torsional shear stress developed on the circular cross section of the helical shaped wire:

$$F = \frac{4\pi}{D} \int_0^{d/2} \tau r^2 dr \quad (5)$$

where r is the radial coordinate along the wire cross section. It is also assumed that the shear strain is linearly distributed along the wire cross section, from what follows the kinematics relation:

$$\gamma = \frac{d}{\pi D^2 N} u \quad (6)$$

where u is the spring displacement.

By combining these equations, and performing the integration, assuming that the wire presents a homogeneous shear stress and phase transformation through the wire cross section, we obtain:

$$F = \frac{\pi d^3}{6D} \left(\frac{Gd}{\pi D^2 N} u - \alpha\beta \right) \quad (7)$$

This equation together with those that describes the volume fraction evolution establishes a proper description of the thermomechanical behavior of SMA helical springs.

The balance of energy for SMA may be written considering a lumped formulation for the helical spring:

$$\rho r - \frac{hA}{L} (T - T_\infty) = c\rho\dot{T} \quad (8)$$

where ρ is the density, L the helical spring total wire length, r a heat source, h the convection coefficient, A the convection surface area, T_∞ the medium temperature and c the specific heat. Temperature variations can be induced in the SMA helical spring through joule effect by the application of an electrical current. Therefore $r = Ri^2$, where R is the SMA linear electric resistance and i is the applied electric current.

4. EXPERIMENTAL PROCEDURE

The characterization of the SMA helical springs is obtained through load-displacement tests using the tensile test device at CEFET/RJ Laboratory of Materials Thermomechanical Behavior (LACTM) shown in Fig. 3a (Aguiar *et al.*,

2008). This device is composed by a rigid frame that has a load cell (Alfa SV-20 with 20 N capacity) fixed at the top. An SMA spring is connected to the load cell and the other end is attached to the rod of a resistive displacement transducer (Gefran PY-1-F-100 with 100 mm span). Both transducers are connected to a data acquisition system (HBM Spider 8). A fluid reservoir is attached to the other end of the transducer rod in order to produce the mechanical loadings. The load is prescribed to the SMA spring by controlling the fluid level of the reservoir which is done by changing the vertical position of a second fluid reservoir that is connected to the first by a tube. This configuration allows one to apply precise loading and unloading conditions to the spring element. Temperature variations are induced in the SMA helical spring through joule effect by the application of an electrical current using a stabilized current source (Minipa MPL-1303). The thermomechanical tests developed are composed by two stages: (1) a mechanical loading-unloading followed by a (2) thermal heating-cooling. The first stage promotes a residual strain that is eliminated during the second stage. Three different levels of loads are considered: 3 N, 3.5 N and 4 N. The heating SMA helical spring to a temperature above A_F is performed by applying an electrical current of 1.2 A. All tests are performed at room temperature (22°C).

The SMA helical is built with NiTi that is in austenitic phase at room temperature. The spring has an external diameter of 6 mm, a wire diameter of 0.75 mm, 20 active coils and an activation temperature in the range of 45-55°C.

Figure 3b shows the spring load-displacement curves for three different load levels revealing the SME. At the beginning of the test, the SMA helical spring is at room temperature (22°C), a situation where austenitic phase is stable. In order to assure that each test is done with a spring where its wire section has a homogeneous austenitic phase distribution, the following process is applied. Initially, all mechanical loads are removed and then, an electric current of 1.2 A is applied to the spring. Finally, the spring is subjected to cooling prescribed in order to allow a thermal equilibrium with the medium. After this initial treatment, a mechanical loading is applied promoting the formation of detwined martensite that remains after the mechanical load removal causing a residual displacement. At this point, an electric current of 1.2 A is applied and the SMA helical spring recovers part of the residual displacement developed during the loading stage. A residual load with a magnitude of approximately 1 N is still present at the end of the unloading as a consequence of the devices attached to the spring (resistive displacement transducer, fluid reservoir, etc). A loading rate of approximately 2.7×10^{-2} N/s is used in the developed tests.

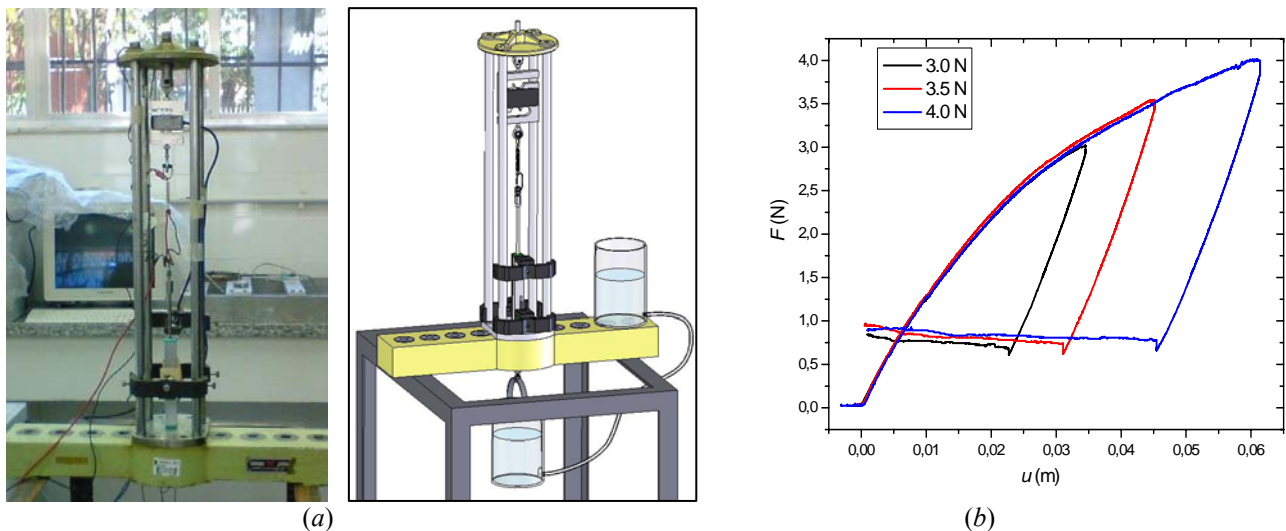


Figure 3. Tensile test device for thermomechanical characterization of the SMA helical springs (a) and experimental data related to the spring load-displacement curve for three load levels (b).

5. NUMERICAL SIMULATIONS

The numerical procedure here proposed is based on the operator split technique (Ortiz *et al.*, 1983) associated with an iterative numerical scheme in order to deal with nonlinearities in the formulation. With this assumption, coupled governing equations are solved from three uncoupled problems: thermal, mechanical and phase transformation behaviors. Therefore, the following moduli are considered:

Thermal Problem - Comprises a transient thermal lumped model with a heat source (joule effect) and surface convection. Energy equation (8) is integrated using a simple Euler method.

Mechanical Problem - Stress and displacement are evaluated from temperature evolution using equations (1), (6) and (7) and a prescribed force.

Phase Transformation Problem - The volumetric fractions of the phases are determined in this problem using equations (2-4).

5.1 Model Verification

Experimental data is used to match parameters of the proposed model. In the beginning of the test, phase transformation does not take place and the initial slope of the load-displacement curve can be used to obtain G . The residual displacement is also employed to match parameters related to phase transformations. Other parameters are obtained from some authors (Paiva, 2004; Toi *et al.*, 2004).

Table 1. SMA helical spring parameters.

Material Parameter	Value	Material Parameter	Value
G_M (GPa)	10.7	τ_S^{crit} (MPa)	20
G_A (GPa)	12.7	τ_F^{crit} (MPa)	100
M_S (°C)	20	C_M (MPa)	8
M_F (°C)	10	C_A (MPa)	13.8
A_S (°C)	40	ρ (Kg/m ³)	6450
A_F (°C)	50	c (J/Kg.K)	465
α (MPa)	250	R (Ω /m)	2

Numerical simulations are now focused on establishing a comparison with experimental tests. It is considered a helical spring with the same characteristics described in the previous section. The SMA helical spring is assumed to be at an initial temperature of 22°C in an austenitic phase ($\beta = 0$) before the loading application. This temperature is similar to the ambient temperature and is between M_S and A_S . A convection coefficient, h , of 10 W/m² °C is used. Numerical simulations are performed with the aid of computational software developed in C programming language.

Figure 4a shows mechanical loading that represents the experimental tests: a mechanical loading-unloading followed by a thermal heating-cooling. Figure 4b show temperature evolution promoted by the application of a electric current. Figure 5 present the force-displacement curves and the volume fraction time evolution for the three loading levels applied in the experimental tests (3 N, 3.5 N and 4 N). The force-displacement curves have the same behavior observed in experimental tests, presenting a residual displacement and a load when the mechanical loading-unloading process is finished. Figures 5b-d allows a better comprehension of the phase transformation process related to this thermomechanical loading process. Initially, martensitic formation takes place due to mechanical loading, changing from austenite to detwinned martensite. The final state for each of the three load levels is the following: $\beta_S = 0.40$ for $F = 3$ N, $\beta_S = 0.62$ for $F = 3.5$ N and $\beta_S = 0.82$ for $F = 4$ N. Afterwards, during the heating-cooling process, there is an austenitic formation during the heating stage.

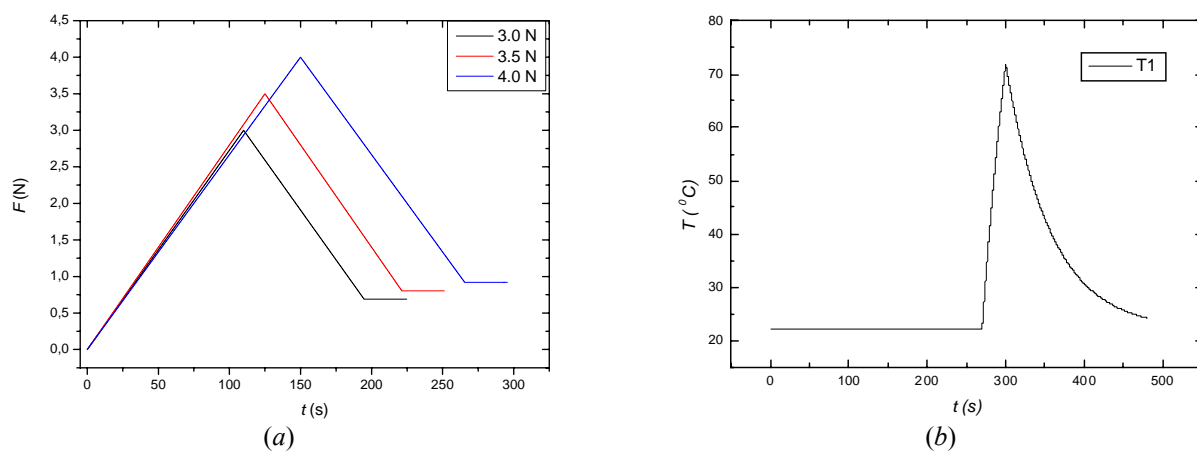


Figure 4. Mechanical loading (a) and temperature evolution (b) for three loading levels. Numerical simulations.

In order to establish a comparison between numerical and experimental tests Fig. 6 presents a direct comparison of the load-displacement curves obtained for three load levels analyzed. Results show that model results are in close agreement with experimental tests.

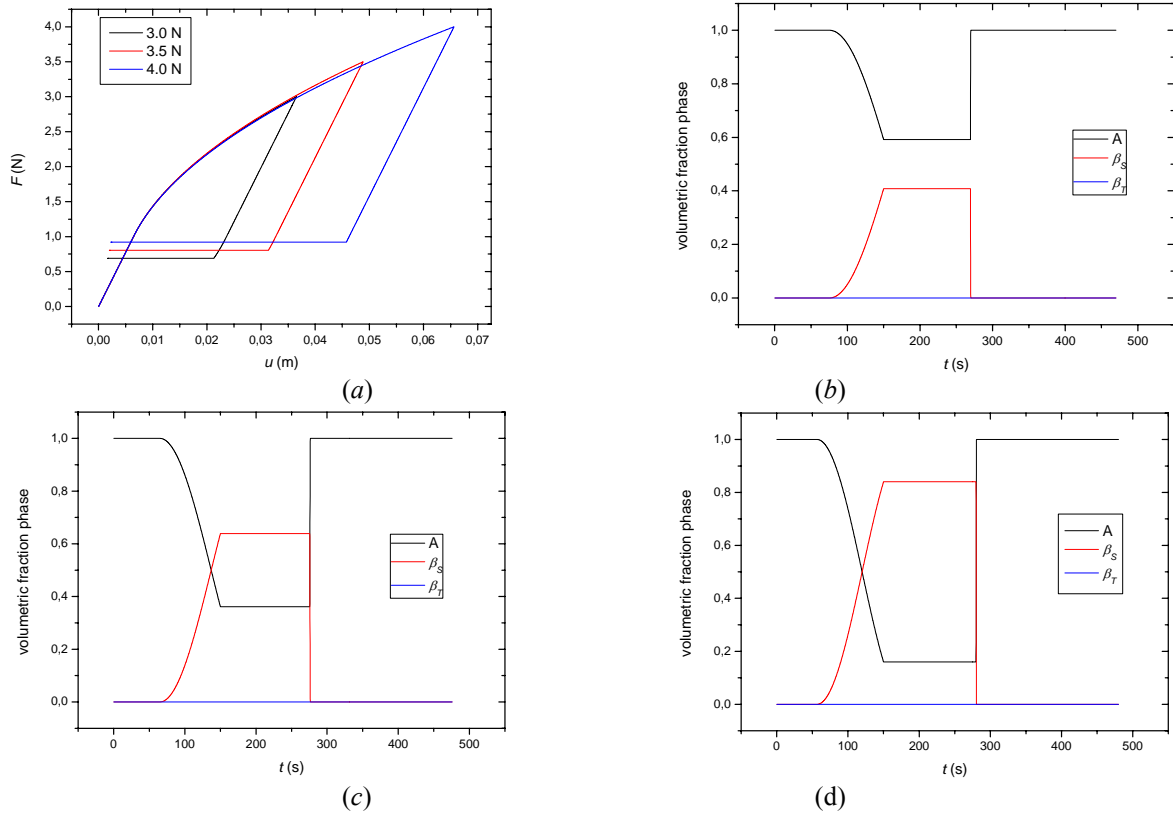


Figure 5. Spring load-displacement curve for three load levels (a). Volume fraction time evolution: (b) $F = 3$ N, (c) $F = 3.5$ N and (d) $F = 4$ N. Numerical simulations.

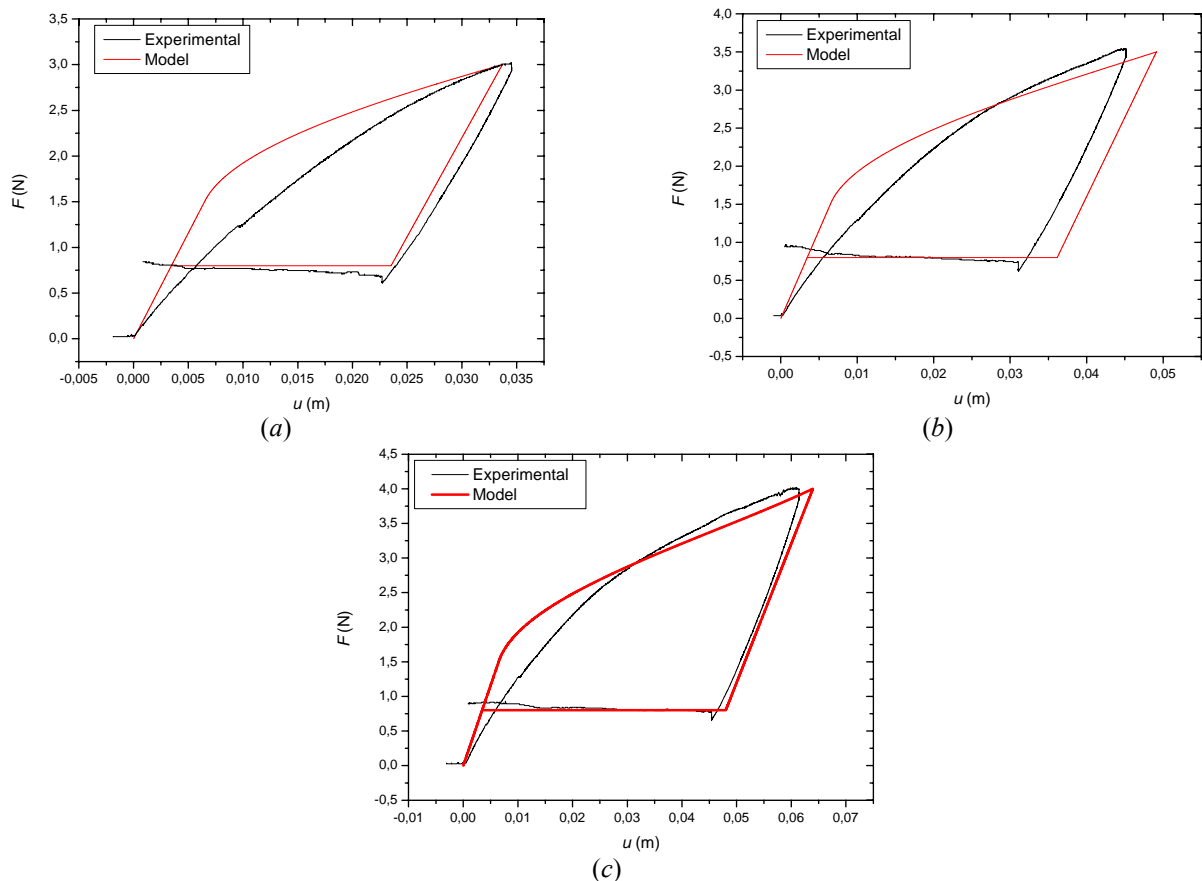


Figure 6. Comparison between experimental and numerical tests of an SMA spring. Load-displacement curve for three load levels. (a) $F = 3$ N, (b) $F = 3.5$ N and (c) $F = 4$ N.

5.2 Performance Analysis

SMA actuator stroke depends on the recovery displacement during the heating stage, which is associated to the amount of martensite induced by stress during mechanical loading. In this section a SMA actuator submitted to a constant load is considered (dead weight). Figure 7 shows force-displacement and displacement evolution curves considering 4 different values of applied constant mechanical loads and $h = 10 \text{ W/m}^2 \text{ C}$, $i = 1.2 \text{ A}$. Figure 8 shows the volumetric phase fractions evolution. The analysis shows that a mechanical load of 1 N is not sufficient to induce detwined martensite formation. For the other three levels the following stroke values are obtained: 2.4 mm for 2 N, 20.7 mm for 3 N and 46.7 mm for 4 N.

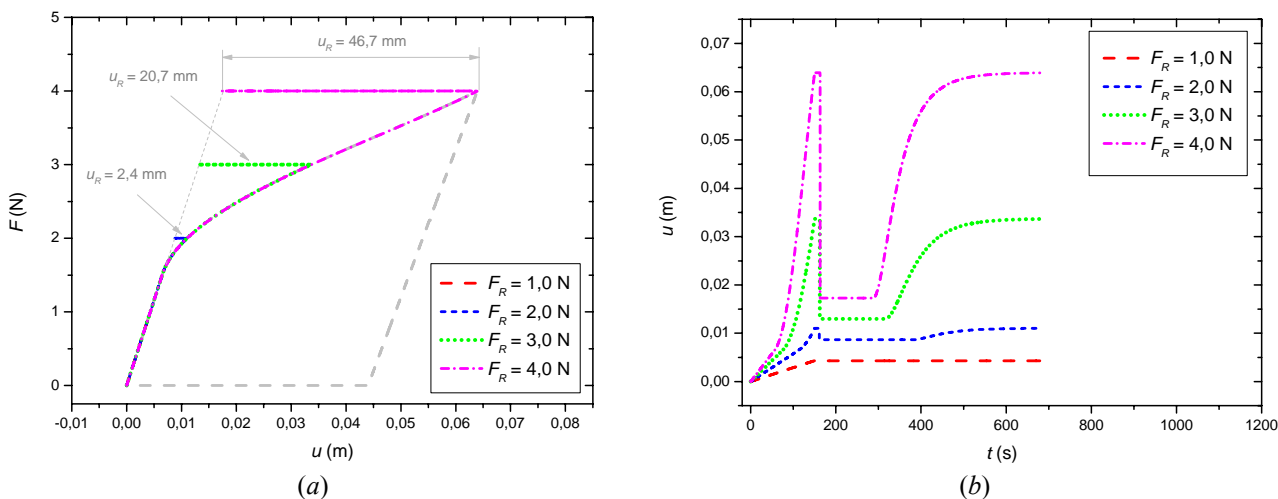


Figure 7. Force-displacement and displacement evolution curves for different values of constant mechanical loads.

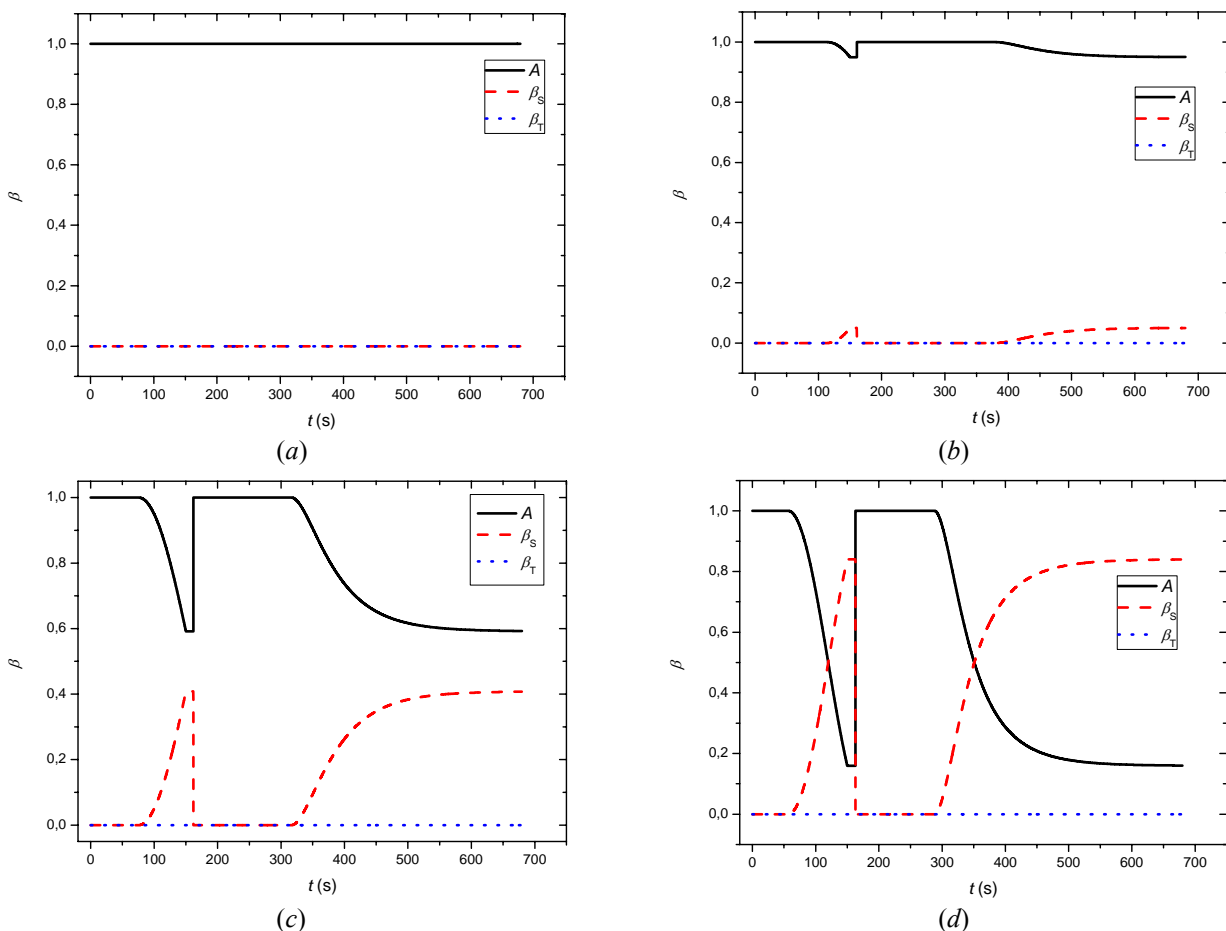


Figure 8. Volumetric phase fractions evolution for 4 different mechanical loading levels: (a) 1 N, (b) 2 N, (c) 3 N, (d) 4 N.

High values of cooling times can be the major drawback for SMA actuators. The actuation time depends directly on the heating and cooling time. During the cooling stage heat must be removed from the SMA material and the simplest method is by convection through a cooling medium as air or a cooling fluid. Several conditions associated to different cooling medium are analyzed using the proposed model to assess the main characteristics of SMA helical springs actuators performance. Five different convection coefficients are considered: 10, 20, 50, 100 and 1000 W/m² °C. The electric current is adjusted to promote a maximum temperature value approximately 70 °C during the heating stage resulting in the following values associated to the 5 convection coefficients: 1.2, 1.35, 1.78, 2.43 and 5 A. In the following analysis the maximum mechanical load of 4 N is considered. Figure 9 shows the temperature evolution for these conditions.

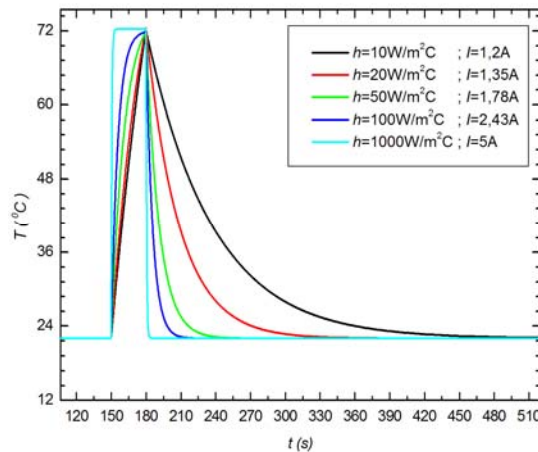


Figure 9. Temperature evolution for 5 different cooling mediums. Numerical simulations.

The analyzed situation considers an applied constant load during the full cycle and the actuation cycle time is associated to the device heating and cooling time. Figure 10 presents the displacement evolution and the volumetric phase fractions for different cooling mediums. The following actuation times can be observed: 420 s for $h = 10 \text{ W/m}^2 \text{ C}$, 220 s for $h = 20 \text{ W/m}^2 \text{ C}$, 87 s for $h = 50 \text{ W/m}^2 \text{ C}$, 44 s for $h = 100 \text{ W/m}^2 \text{ C}$ and 3 s for $h = 1000 \text{ W/m}^2 \text{ C}$. Table 2 presents the data associated with the performance of the SMA device.

Table 2. Data associated with the performance of SMA helical springs actuators.

	$h \text{ (W/m}^2\text{C)}$				
	10	20	50	100	1000
Heating velocity (recovery) (mm/s)	1.56	1.56	1.56	1.56	23.4
Cooling velocity (mm/s)	0.11	0.21	0.54	1.06	15.6
Actuation velocity (mm/s)	0.21	0.37	0.80	1.26	18.7
Actuation Frequency (Hz)	0.002	0.004	0.009	0.014	0.20

For severe cooling conditions, as $h = 1000 \text{ W/m}^2\text{C}$, the SMA helical springs actuators response is similar to commercial actuation devices as piezoelectric actuators. Table 3 presents a comparison between data for the SMA device analyzed and two commercial piezoelectric actuators (Physik Instrumente, 2009). The major advantage of SMA devices is the capability to generate large forces and displacements with a lower weight and cost.

Table 3. Data for SMA device and two commercial piezoelectric actuators (Physik Instrumente, 2009).

	SMA device	M-228 (piezoelectric)	M-674 (piezoelectric)
Stroke (mm)	46.7	10	50
Maximum Force	4	20	7
Current (A)	5	0.25 (A/phase)	1.25
Temperature (°C)	20 – 50	20 – 65	20 – 50
Maximum Velocity (mm/s)	18.7	1.5	450
Frequency (Hz)	0.21	0.15	9.09
Mass (g)	4.6	230	100
Cost (US \$)	20	800	1400

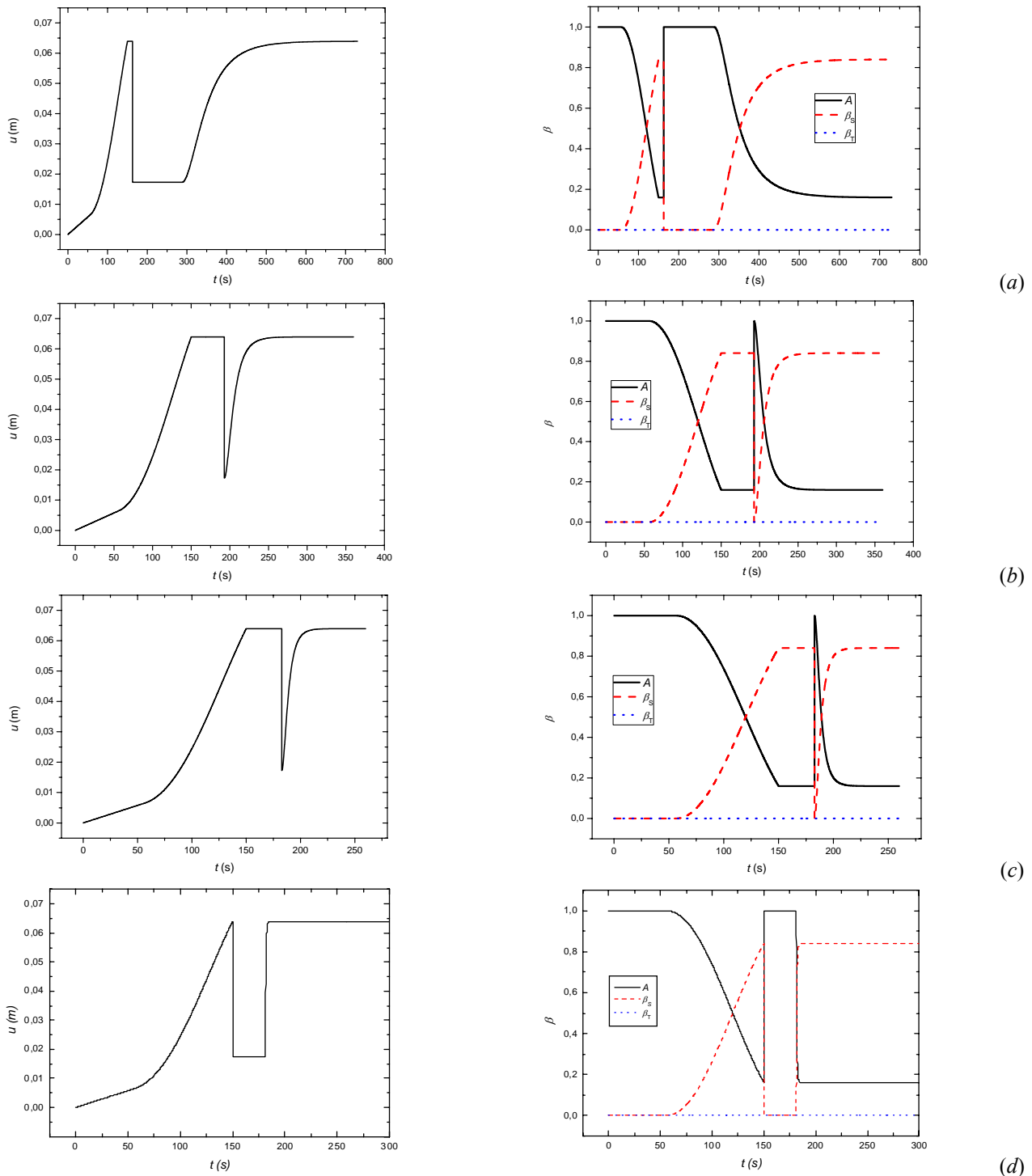


Figure 10. Displacement and phase fractions for different media: (a) 10, (b) 50, (c) 100 and (d) 1000 W/m² C.

6. CONCLUSION

Shape memory alloys (SMAs) are metallic materials that have the capability to generate large strains and loads associated to phase transformation induced by stress or temperature. Because of such properties, SMAs have found a number of applications in different areas as actuation systems. This contribution analyses the quasi-static response of a linear actuator with SMA helical springs. A one-dimensional constitutive model which assumes the kinetics of the phase transformation is used to describe the thermomechanical shear behavior of SMA helical springs. A numerical method based on the operator split technique is employed in order to deal with nonlinearities in the formulation. An experimental apparatus is developed in order to characterize the thermomechanical behavior of SMA helical springs through load-displacement tests. Numerical results show that the proposed model is in close agreement with experimental data obtained and can be used to design and predict the response of SMA helical spring actuators. Several

conditions are analyzed with the proposed model to assess the main characteristics of SMA helical springs actuators performance.

7. ACKNOWLEDGEMENTS

The authors would like to acknowledge the support of the Brazilian Research Agency CNPq.

8. REFERENCES

- Aguiar, R.A.A., Pacheco, P.M.C.L., Basileu, R., Savi, M.A., 2008; "Experimental Analysis of a Single-Degree of Freedom Shape Memory Alloy Oscillator", *CONEM2008 - V Congresso Nacional de Engenharia Mecânica*.
- Brinson, L.C., 1993, "One Dimensional Constitutive Behavior of Shape Memory Alloys: thermomechanical derivation with non constant material functions and redefined martensite internal variable", *Journal of Intelligent Material Systems and Structures*, n. 4, pp. 229-242.
- Chang-jun,Q., Pei-sun, M. e Qin, Y., 2004. "A prototype micro-wheeled-robot using SMA actuator", *Sensors and Actuators*, A 113, pp.94-99.
- Denoyer, K.K., Scott Erwin, R. & Rory Ninneman, R., 2000, "Advanced smart structures flight experiments for precision spacecraft", *Acta Astronautica*, v.47, pp.389-397.
- Elzey, D.M., Sofla, A.Y.N. e Wadley, H.N.G., 2005. "A shape memory-based multifunctional structural actuator panel", *International Journal of Solids and Structures*, 42, pp.1943-1955.
- Hodgson, D. E., Wu, M. H. and Biermann, R. J., 1992. "Shape Memory Alloys", *ASM Handbook*, v. 2, p. 887-902.
- Jackson, C.M., Wagner, H.J. and Wasilewski, R.J., 1972, "55-Nitinol - The alloy with a memory: Its physical metallurgy, properties, and applications", NASA-SP-5110.
- Kibirkstis, E., Liaudinskas, R., Pauliukaitis, D. and Vaitasius, K., 1997, "Mechanisms with shape memory alloy", *Journal de Physique IV*, C5, pp.633-636.
- La Cava, C.A.P.L., Pacheco, P.M.C.L. e Savi, M.A., 2000. "Modelagem de um Dispositivo de Pré-Carga com Memória de Forma para Juntas Flangeadas", *CONEM 2000 - Congresso Nacional de Engenharia Mecânica*, Natal-RN.
- Machado, L.G. and Savi, M.A., 2003, "Medical applications of shape memory alloys", *Brazilian Journal of Medical and Biological Research*, v.36, n.6, pp.683-691.
- Manach, P-Y. and Favier, D., 1977, "Shear and tensile thermomechanical behavior of near equiatomic NiTi alloy", *Materials Science & Engineering A*, v.222, pp.45-57.
- Ortiz, M., Pinsky, P.M. and Taylor, R.L., 1983, "Operator split methods for the numerical solution of the elastoplastic dynamic problem", *Computer Methods of Applied Mechanics and Engineering*, v.39, pp.137-157.
- Pacheco, P.M.C.L. and Savi, M.A., 1997, "A non-explosive release device for aerospace applications using shape memory alloys", *COBEM 97 - Proceedings of XIV the Brazilian Congress of Mechanical Engineering*, Bauru.
- Paiva, A., 2004, "Modeling of Thermomechanical Behavior of Shape Memory Alloys", Ph.D. Thesis, PUC-Rio, Department of Mechanical Engineering (in portuguese).
- Physik Instrumente (PI), 2009, "Linear Actuator for Precision Motion Control", "<http://www.physikinstrumente.com>", captured in May, 2009.
- Rogers, C.A., 1995, "Intelligent Materials", *Scientific American*, September, pp.122-127.
- Savi, M. A. and Braga, A. M. B., 1993, "Chaotic vibrations of an oscillator with shape memory", *Journal of the Brazilian Society of Mechanical Sciences and Engineering*, v.XV, n.1, pp.1-20.
- Shin, D.D., Mohanchandra, K. P. e Carman. G.P., 2005. "Development of hydraulic linear actuator using thin film SMA", *Sensors and Actuators A* 119, pp.151-156.
- Tobushi, H. and Tanaka, K., 1991, "Deformation of a shape memory alloy helical spring - (Analysis based on stress-strain-temperature relation)", *JSME International Journal Series I - Solid Mechanics Strength of Materials*, v.34, n.1, pp.83-89.
- Toi, Y., Lee, J-B. and Taya, M., 2004, "Finite element analysis of superelastic, large deformation behavior of shape memory alloy helical springs", *Computer & Structures*, v.82, pp.1685-1693.
- van Humbeeck, J., 1999, "Non-medical applications of shape memory alloys", *Materials Science and Engineering A*, v.273-275, pp.134-148.
- Webb, G., Wilson, L., Lagoudas, D.C. and Rediniotis, O., 2000, "Adaptive control of shape memory alloy actuators for underwater biomimetic applications", *AIAA Journal*, v.38, n.2, pp. 325-334.
- Williams, K., Chiu, G. and Bernhard, R., 2002, "Adaptive-passive absorbers using shape-memory alloys", *Journal of Sound and Vibration*, v.249, n.5, pp.835-848.
- Zhang, X.D., Rogers, C.A. & Liang, C., 1991, "Modeling of Two-Way Shape Memory Effect", *ASME - Smart Structures and Materials*, v.24, pp.79-90.

9. RESPONSIBILITY NOTICE

The authors are the only responsible for the printed material included in this paper.